J. Fluid Mech. (2006), *vol.* 547, *pp.* 267–296.
doi:10.1017/S0022112005007263 Printed in the United Kingdom

An improved integral model for plane and round turbulent buoyant jets

By P. C. YANNOPOULOS

Environmental Engineering Laboratory, Department of Civil Engineering,
University of Patras, 265 00 Patras, Greece

(Received 3 August 2004 and in revised form 11 July 2005)

The integral momentum and tracer equations for the mean motion with the turbulence contribution in momentum and tracer fluxes are integrated on the centreline of either plane or round buoyant jets, using suitable assumptions for the spreading coefficients and a closing function, and unified first- and second-order solutions are derived in the entire buoyancy range for mean axial velocities and mean concentrations. Comparisons to experimental data in the literature validate the model and show that second-order solutions deviate less than first-order solutions. Both types are used in conjunction with the integral continuity and kinetic energy equations for the mean motion to determine the variation of the local Richardson and Froude numbers, dispersion ratio, bulk dilution, dilution ratio, entrainment coefficient and mean velocity, kinetic energy flux and its gradient for the mean motion; and the variations of these quantities are evaluated using reported experimental or theoretical data. Finally, the variation of the product of kinetic energy flux and the local Richardson number is examined and a universal constant for both plane and round buoyant jets is revealed, leading to a unified definition of the local Richardson number, which is independent of the flow and mixing geometry and could be useful. Simple computational programming and good overall agreement make the proposed model a very promising tool for laboratory and field studies, outfall design and validation of numerical models.

1. Introduction

The outfall discharge of wastewater or warm water into surface-water bodies or the chimney release of air pollutants and volcanic gas eruptions into the atmosphere are associated with complicated turbulent buoyant-jet phenomena; in depth knowledge of these relationships is required for environmental quality assessment and design optimization of the discharge structures, minimizing cost and providing environmental protection.

The integral method is popular for solving buoyant-jet problems. It is based on simplified partial differential equations (continuity, momentum and tracer transport) by adopting commonly used approximations for such types of flow and mixing phenomena. The equations are integrated on the jet cross-section, applying the similarity assumption and actual boundary conditions to yield a system of ordinary differential equations, and then the system may be solved either analytically or numerically. There are two approaches to the final integration of the set of ordinary differential equations: (*a*) using the entrainment concept (Morton, Taylor & Turner 1956) and making suitable assumptions for the entrainment coefficient (Morton 1959; List & Imberger

1973; Turner 1986; Lee & Cheung 1990; Davidson, Gaskin & Wood 2002; Jirka 2004); and (*b*) using the spreading concept (Abraham 1963) and making suitable assumptions for the spreading coefficient (Noutsopoulos & Yannopoulos 1987, hereinafter referred to as NY; Yannopoulos & Noutsopoulos 1990, hereinafter referred to as YN). These procedures have been extensively discussed and compared in the literature (Jirka, Abraham & Harleman 1975). A major advantage of the integral method is the formulation of a simple problem, employing closure assumptions based on semi-empirical approximations without the need for assigning detailed turbulence characteristics. Integral solutions usually provide an acceptable level of accuracy, sometimes resulting in unified analytical expressions; they are widely used in laboratory and field studies, as well as in validating complex numerical models. Jirka (2004) describes in detail the use of the integral method in buoyant-jet flows and its applicability limits; he and his co-workers have formulated and validated the Corjet integral model, which has been incorporated in the Cormix model (Jirka, Doneker & Hinton 1996).

The majority of integral models consider only the mean mass and momentum fluxes in the set of conservation equations. These endeavours are referred to as first-order integral models to distinguish them from those that take into account the turbulence contribution to the mass and momentum fluxes; because of improved accuracy, the latter models have been termed second-order integral models. Few models treat the turbulence contribution as a fixed percentage of the related mean flux (Wood, Bell & Wilkinson 1993; Davidson *et al.* 2002) and only the model by Wang & Law (2002) is an original second-order as it takes into account the variable contribution of the turbulent mass and momentum fluxes and considers the change in the concentration-to-velocity width ratio from jet to plume.

The spreading concept is adopted in this paper and a closure assumption concerning a function of the spreading coefficients is proposed; this enables integration of the momentum and tracer equations and provides unified solutions over the entire Froude number range regarding centreline distributions of the mean axial velocity and mean concentration for either plane or round vertical turbulent buoyant jets in a quiescent ambient fluid of uniform density. Additionally, both the variation of the concentration-to-velocity width ratio and the variable turbulence contribution to mass and momentum fluxes are considered in the entire buoyancy range. Consequently, the present work could be considered a second-order integral model or simply a second-order approach (SOA), since it yields better accuracy than models using the first-order approach (FOA), reducing absolute errors below 10 %. In order to reach the SOA solutions, however, FOA solutions are required. Solutions obtained in this study are compared with experimental data available in the literature, and additional significant implications are drawn and discussed.

2. Theoretical considerations

2.1. *Governing equations*

A two-dimensional or three-dimensional flow and mass transport configuration for a plane or round vertical turbulent buoyant jet in steady-state conditions in a Cartesian (O, xyz) or cylindrical $(O, r\varphi z)$ coordinate system, respectively, with the z-axis vertical, is shown with all pertinent quantities identified in figure 1. The line or point source is located on the system y-axis and origin O, respectively; the z-axis coincides with the jet centreline and the flow and concentration fields are symmetrical with respect to the (z, x) and (z, y)-planes. The fluid densities are ρ_0 at the jet exit and ρ_a $(\rho_a \geqslant \rho_0)$ at the ambient, while ρ is the density at a point (x, y, z) of the flow field; subscripts

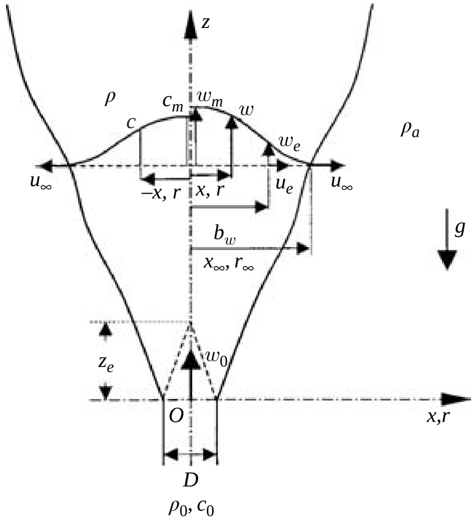

FIGURE 1. Definition of a plane or round vertical buoyant jet.

0 and a denote jet-exit and ambient-fluid locations. The density differences are considered small enough, so that $\rho_a/\rho_0 \approx 1$. For the analytical description of the mean flow characteristics, usually accepted assumptions are considered, including: (a) the Boussinesq's approximation made for small initial density differences, $\Delta\rho_0 = \rho_a - \rho_0 \ll \rho_0 < \rho_a$; ($b$) the Prandtl's boundary-layer-type approximation; (c) negligible molecular viscosity terms and; (d) no swirl. Taking into consideration the symmetry of the flow with respect to the (z, x)- and (z, y)-planes and the conservation principles of volume, momentum, tracer-mass and mean kinetic energy for steady turbulent flow, the following synoptic forms of four partial differential equations are obtained:

continuity

$$\frac{\partial(r^i w)}{\partial z} + \frac{\partial(r^i u)}{\partial r} = 0, \tag{2.1}$$

momentum

$$\frac{\partial}{\partial z}[r^i(w^2 + w'^2)] + \frac{\partial(r^i wu)}{\partial r} = g_0' r^i c + \frac{\partial(r^i \tau_{zr})}{\rho_0 \partial r}, \tag{2.2}$$

conservation of tracer

$$\frac{\partial}{\partial z}[r^i(wc + w'c')] + \frac{\partial(r^i uc)}{\partial r} = -\frac{\partial(r^i u'c')}{\partial r}, \tag{2.3}$$

conservation of mean kinetic energy

$$\frac{\partial(r^i w\omega)}{\partial z} + \frac{\partial(r^i u\omega)}{\partial r} = g_0' r^i wc - r^i f, \tag{2.4}$$

where $i = 0$ or 1 for a plane or round buoyant jet, respectively; w is the axial mean velocity component (z-direction), u the transverse mean velocity component (radial for a round buoyant jet), and $r = \sqrt{x^2 + iy^2}$ the transverse distance from the jet centreline (jet cross-section radius for a round buoyant jet); $g_0' = g(\rho_a - \rho)/(\rho_a - \rho_0) = g\Delta\rho_0/\rho_0$ is the apparent acceleration due to gravity; τ_{zr} is the mean turbulent shear stress on the (z, r)-plane and parallel to the z-axis; $c = (\rho_a - \rho)/(\rho_a - \rho_0) = \Delta\rho/\Delta\rho_0$ is the relative mean concentration of tracer; w'^2, $w'c'$, $u'c'$ are the local mean axial velocity

Flux	Definition	Initial value
Volume	$\mu = \int_A w\,\mathrm{d}A$	$\mu_0 = A_0 w_0$
Momentum	$m = \int_A (w^2 + w'^2)\,\mathrm{d}A = \lambda_M \int_A w^2\,\mathrm{d}A$	$m_0 = A_0 w_0^2$
Weight deficit	$\zeta = \int_A g'\,\mathrm{d}A = g'_0 \int_A c\,\mathrm{d}A$	$\zeta_0 = A_0 g'_0$
Buoyancy	$\beta = g'_0 \int_A (cw + c'w')\,\mathrm{d}A = \lambda_B g'_0 \int_A cw\,\mathrm{d}A$	$\beta_0 = g'_0 \mu_0$
Kinetic energy for mean motion	$\varepsilon = \int_A w\omega\,\mathrm{d}A = \lambda_E \int_A \frac{1}{2} w^3\,\mathrm{d}A$	$\varepsilon_0 = \frac{1}{2} A_0 w_0^3$
Kinetic energy f-terms	$\varepsilon_f = \int_A f\,\mathrm{d}A$	$\varepsilon_{f0} = 0$

TABLE 1. Kinematic fluxes and their initial values for vertical buoyant jets.

and tracer fluxes due to turbulence fluctuations of w, u and c; $\omega = (w^2 + u^2)/2$ is the kinetic energy for the mean motion based on mean velocities; and f represents the remaining terms of the conservation of the mean kinetic energy equation. The following boundary conditions have to be satisfied,

$$\left.\begin{aligned} &\text{for } r = 0 \quad u = 0, \quad w = w_m, \quad c = c_m, \quad \tau_{zr} = 0, \quad u'c' = 0, \quad f = 0, \\ &\text{for } r \to \infty \quad u = u_\infty, \quad w = 0, \quad c = 0, \quad \tau_{zr} = 0, \quad u'c' = 0, \quad f = 0, \end{aligned}\right\} \tag{2.5}$$

and the integral method, with the similarity assumption, which is well substantiated in the zone of established flow (ZEF), is used in this work to reduce the four partial differential equations to four ordinary differential equations. Under this assumption, one scale for a mean flow variable ϕ (mean axial velocity w or mean concentration c) and one scale for the lateral length b are sufficient to make the dimensionless expressions of the mean flow variables unique functions of a geometrical variable only. The centreline value of the corresponding variable and the nominal lateral width b_ϕ are selected as the reference values, and the similarity function is well represented by the Gaussian distribution (Reichardt 1941; Albertson *et al.* 1950; Rouse, Yih & Humphreys 1952; Papanicolaou & List 1988; Jirka 2004) in both round (three-dimensional) and plane (two-dimensional) geometries. Therefore, the dimensionless mean axial velocity and concentration profiles may be expressed as,

$$\frac{\phi}{\phi_m} = \exp\left(-\frac{r^2}{b_\phi^2}\right), \tag{2.6}$$

where $r^2 = x^2 + iy^2$ (when $i = 0$, $r \equiv x$ is the transverse distance and when $i = 1$, r is the radial distance); and the lateral width b_ϕ is the length scale of property ϕ defined by the point on the profile at which the value is 1/e times the maximum value (figure 1). For the limiting cases of simple jets and pure plumes, where self-similarity holds, b_ϕ is proportional to the axial distance z ($b_\phi = K_\phi z$, where K_ϕ is the spreading rate coefficient); however, this is not generally true for buoyant jets, where the spreading coefficient may vary with distance z (NY; Papanicolaou & List 1988; Wang & Law 2002).

The kinematic fluxes normalized by their initial values at the jet exit are defined in table 1 and are useful in the integral method and for dimensional considerations. The following notes should be used in conjunction with this table: $g' = g'_0 c$; $c_0 = 1$; for $i = 0$, slot width D and flow cross-sectional area per unit slot length A, $\mathrm{d}A/A_0 = 2\mathrm{d}x/D = 2\mathrm{d}n_x$; for $i = 1$, nozzle diameter D and flow cross-sectional area A, $\mathrm{d}\,A/A_0 = 4\mathrm{d}r^2/D^2 = 4\mathrm{d}n_r^2$; $A_0 = (\pi/4)^i D^{1+i}$; $n_x = x/D$ and $n_r = r/D$ are non-dimensional distances from the jet centreline in the x and r directions; and subscript 0 denotes value at the jet exit.

For a buoyant jet, the flow is determined uniquely by the three initial fluxes of volume μ_0, momentum m_0 and, buoyancy β_0, and the vertical distance z from the jet exit, which form a set of four independent variables; a completely equivalent set of independent variables are the characteristic length scale D, the exit jet velocity w_0, the apparent acceleration due to gravity g'_0, and the distance z. Both sets contain only kinematic dimensions, and formal dimensional analysis would indicate that there are only two truly independent dimensionless groups, which may be formed from the two sets of variables. Selecting the first set, the two groups are $R_0 = \mu_0^{(3+i)/(1+i)} \beta_0 m_0^{-(3+2i)/(1+i)}$ and z/L_m, where R_0 is defined as the initial Richardson number and L_m is the characteristic length scale defined by Fischer *et al.* (1979) as $L_m = m_0 \beta_0^{-2/3}$ when $i = 0$ and $L_m = m_0^{3/4} \beta_0^{-1/2}$ when $i = 1$; and using the second set, they are $F_0 = w_0 (g'_0 D)^{-1/2}$ and $Z = (z/D) F_0^{-4/(3+i)}$, where F_0 is the initial densimetric Froude number. It must be noted that $R_0 = (\pi/4)^{i/2} F_0^{-2}$, $L_m = D(\pi/4)^{i/4} F_0^{4/(3+i)}$ and $z/L_m = (\pi/4)^{-i/4} Z$; therefore, the variations of mean flow and mixing quantities can be completely presented in terms of Z and F_0, or alternatively z/L_m and F_0, as the non-dimensional independent variables.

2.2. *Integration of equations*

Using the prescribed boundary conditions (2.5) and Gaussian distribution profiles (2.6), the four partial differential equations (2.1) to (2.4) are integrated on the jet cross-section, and the following set of ordinary differential equations is derived:

$$\frac{\mathrm{d}\mu}{\mathrm{d}z} = \frac{\mathrm{d}}{\mathrm{d}z}\left[\left(\sqrt{\pi}\, b_w\right)^{1+i} w_m\right] = -2(\pi b_w)^i u_e, \tag{2.7}$$

$$\frac{\mathrm{d}m}{\mathrm{d}z} = \frac{\mathrm{d}}{\mathrm{d}z}\left[\lambda_M \left(\sqrt{\pi/2}\, b_w\right)^{1+i} w_m^2\right] = \zeta = g'_0 (\sqrt{\pi}\, b_c)^{1+i} c_m, \tag{2.8}$$

$$\frac{\mathrm{d}}{\mathrm{d}z}\left(\frac{\beta}{g'_0}\right) = \frac{\mathrm{d}}{\mathrm{d}z}\left[\lambda_B \left(\sqrt{\pi}\frac{b_w b_c}{\sqrt{b_w^2 + b_c^2}}\right)^{1+i} w_m c_m\right] = 0, \tag{2.9}$$

$$\frac{\mathrm{d}\varepsilon}{\mathrm{d}z} = \frac{\mathrm{d}}{\mathrm{d}z}\left[\tfrac{1}{2}\lambda_E (\sqrt{\pi/3}\, b_w)^{1+i} w_m^3\right] = \beta_0 - (\pi r_\infty)^i u_\infty^3 - \varepsilon_f, \tag{2.10}$$

where μ, m, ζ, β and ε are the volume, momentum, weight deficit, buoyancy and kinetic energy fluxes for the mean motion, respectively, defined in table 1; the $(\pi r_\infty)^i u_\infty$ value has been replaced by $(\pi b_w)^i u_e$ in (2.7) to keep the entraining volume constant, thus $u_\infty = (b_w/r_\infty) u_e$; u_e and u_∞ are transverse mean velocities at distances b_w and r_∞ from the jet centreline; $r_\infty \approx 0.18z$ is the entire width of the round buoyant jet, which is taken approximately equal to the optical boundary (NY); b_w and b_c are nominal lateral widths for the velocity and concentration fields; λ_M and λ_B are factors, considered variable from jets to plumes, used to account for the turbulent flux contributions in momentum and buoyancy, while λ_E is a factor for the mean cross-stream velocity contribution in the kinetic energy flux for the mean motion.

Following the spreading concept previously described, (2.9) is integrated with respect to z taking into consideration the corresponding flux definition (table 1) and then solved for c_m to obtain:

$$c_m = \lambda_B^{-1}\left(\pi\frac{b_w b_c}{2}\right)^{-(1+i)/2} Y\mu_0 w_m^{-1}, \tag{2.11}$$

where $Y=[(b_w^2+b_c^2)/(2b_w b_c)]^{(1+i)/2}=[(K_w^2+K_c^2)/(2K_w K_c)]^{(1+i)/2}$ is a function of the spreading coefficients; $b_\phi = K_\phi z$ ($\phi \equiv w$ or $\phi \equiv c$) and K_ϕ is generally a function of z for prescribed initial conditions. Replacing this expression of c_m in the momentum equation (2.8), integrating in the ZEF between z_e and $z > z_e$ (z_e approximates the core length), or equivalently between Z_e and Z (Z_e is the value of Z at the core end), dividing both sides of the resulting equation by $m_0^{3/2}$ (where m_0 is the initial momentum at the jet exit, table 1), and solving for the velocity ratio w_m/w_0, irrespective of the variation of b_w with z or Z, the following expression is obtained,

$$\frac{w_m}{w_0} = \frac{2^{-i/2}}{\sqrt{\lambda_M}}\left(\frac{\pi}{2}\right)^{(i-1)/4}\left(\frac{b_w}{D}\right)^{-(1+i)/2}\left[M_1 + \tfrac{3}{2}2^{i/2}\left(\frac{\pi}{2}\right)^{(1-i)/4} F\left(Z^{(3+i)/2}\right)\right]^{1/3} \tag{2.12}$$

after the following substitutions were made:

$$F\left(Z^{(3+i)/2}\right) = \int_0^Z f\left(Z^{(1+i)/2}\right)\mathrm{d}Z, \quad f\left(Z^{(1+i)/2}\right) = \frac{\lambda_M^{1/2}}{\lambda_B} Y(2K_c Z)^{(1+i)/2}, \tag{2.13}$$

$$M_1 = \left(\frac{m_e}{m_0}\right)^{3/2} - \tfrac{3}{2}2^{i/2}\left(\frac{\pi}{2}\right)^{(1-i)/4} F\left(Z_e^{(3+i)/2}\right), \tag{2.14}$$

where $F(Z^{(3+i)/2})$ is the integral function of $f(Z^{(1+i)/2})$, giving the integral of the function from 0 to Z; m_e is the momentum flux at z_e; λ_M and λ_B are factors introducing the turbulent flux contribution into momentum and buoyancy; and M_1 may be considered as the zone of flow establishment (ZFE) memory parameter, as it carries the ZEF effects. In order to obtain an analytical expression for the centreline axial velocity distribution from (2.12) and consequently for the centreline concentration distribution from (2.11), two conditions are required: (*a*) determination of M_1, or m_e and Z_e, and (*b*) determination of the function $f(Z^{(1+i)/2})$. According to YN and NY, after applying a specific first-order model for the ZFE, the following functions were found to approximate M_1:

for plane buoyant jets ($i=0$) *and* $F_0 \geqslant F_p \approx 2.65$,

$$M_1 = 1 + 1.6F_0^{-2}, \tag{2.15}$$

for round buoyant jets ($i=1$) *and* $F_0 \geqslant F_p \approx 2.50$,

$$M_1 = 1 + 3.0F_0^{-2}, \tag{2.16}$$

where F_p is the plume-region limiting value of the local Froude number defined below; in addition, for $F_0 < F_p$ values of $M_1 = 1.23$ for plane plumes and $M_1 = 1.48$ for round plumes have been given. It is noted that the spreading rate coefficients used in the ZFE model to obtain forms (2.15) and (2.16) were mean values of the corresponding coefficients valid in the ZEF for jet-like and plume-like behaviour. As shown by equation (2.12) and approximations (2.15)and (2.16), the memory effect entered by M_1 in the ZEF fades quickly for increasing distances $Z > Z_e$, and because interest is mainly focused on the ZEF, where the ZFE characteristics play an insignificant role, the choice of the simplest model for the ZEF simulations seems to be preferable. Although alternative ZFE models could be used with SOA, the suggested model is

Authors	Jet			Plume		
	K_{wj}	K_{cj}	λ_j	K_{wp}	K_{cp}	λ_p
Plane						
Ramaprian & Chandrasekhara (1985)	0.135	0.201	1.49			
Ramaprian & Chandrasekhara (1989)				0.132	0.160	1.21
Round						
Noutsopoulos & Yannopoulos (1987)	0.100	0.120	1.20	0.120	0.120	1.00
Papanicolaou & List (1988)	0.104	0.126	1.21	0.105	0.112	1.07
Shabbir & George (1994)				0.131	0.121	0.92
Webster, Roberts & Ra'ad(2001)	0.107	0.140	1.31			
Wang & Law (2002)	0.106	0.129	1.22	0.105	0.109	1.04

TABLE 2. Values of K_w, K_c and $\lambda = b_c/b_w = K_c/K_w$ for round and plane jets and plumes based on experiments conducted during the last two decades.

compatible with the results obtained by application of non-dimensional analysis to the ZEF, where the non-dimensional mean flow and mixing properties depend on both Z and F_0; for engineering purposes (when $z/D \geqslant 10$), where M_1 contributes very little to the variation of axial velocity and concentration distributions, $M_1 \approx 1$. The determination of the function $f(Z^{(1+i)/2})$ is given in the following section.

2.3. *Sensitivity analysis*

Applying the identity,

$$(b_w - b_c)^2 = b_w^2 + b_c^2 - 2b_w b_c, \tag{2.17}$$

and rearranging terms with regard to equations (2.11) and (2.13), the following forms are derived:

$$Y = \left(\frac{b_w^2 + b_c^2}{2b_w b_c}\right)^{(1+i)/2} = \left(\frac{K_w^2 + K_c^2}{2K_w K_c}\right)^{(1+i)/2} = \left(\frac{1+\lambda^2}{2\lambda}\right)^{(1+i)/2} = \left[1 + \frac{(1-\lambda)^2}{2\lambda}\right]^{(1+i)/2} \tag{2.18}$$

where $\lambda = b_c/b_w = K_c/K_w$ varies from jet to plume behaviour, as shown in table 2. It is observed that the right-hand side of (2.18) can be approximated to unity; consequently,

$$Y = \left(\frac{b_w^2 + b_c^2}{2b_w b_c}\right)^{(1+i)/2} = \left(\frac{K_w^2 + K_c^2}{2K_w K_c}\right)^{(1+i)/2} \cong 1, \tag{2.19}$$

and the error introduced by approximation (2.19) is $Y_{er} = [1 + 0.5\lambda^{-1}(1-\lambda)^2]^{(1+i)/2} - 1$. Noting that $\lambda = 1 + \epsilon$ (where $0 \leqslant \epsilon < 1$) $Y_{er} \sim O(\epsilon^2)$, indicating the small error committed by this approximation; in fact, according to values of λ reported in table 2, the maximum error that could be introduced in (2.18) would be 4.0 %, and since these errors are very small, approximation (2.19) may be adopted at least for FOA modelling. It should also be noted that use of this assumption is not necessary in the computation process of SOA and, according to Wang & Law (2002), for second-order approximations, factor λ_M remains essentially constant ($\lambda_M \approx 1.1$) for round buoyant jets; the same value is taken for plane buoyant jets, as it can be deduced from the plane turbulent jet measurements of Ramaprian & Chandrasekhara (1985). Factor λ_B may be calculated according to Wang & Law (2002) by the relationship:

$$\lambda_B = \lambda_{Bj} - \left(\lambda_{Bj} - \lambda_{Bp}\right)\frac{R}{R_p}, \tag{2.20}$$

where R is the local Richardson number defined in a following section and R_p is its limiting value in the plume region; according to Ramaprian & Chandrasekhara (1985, 1989) and Wang & Law (2002), $\lambda_{Bj} = 1.04$ and 1.076 for plane and round jets, while $\lambda_{Bp} = 1.18$ and 1.15 and $R_p = 0.28 \pm 0.04$ and 0.341 for plane and round plumes, respectively. A similar form of interpolation is followed for the concentration-to-velocity width ratio $\lambda = K_c/K_w$, which according to Wang & Law (2002) is given by the relationship:

$$\lambda = \frac{K_c}{K_w} = \lambda_j - (\lambda_j - \lambda_p)\left(\frac{R}{R_p}\right)^{3/4}, \tag{2.21}$$

where $\lambda_j = 1.50$ and 1.23, for plane and round jets, and $\lambda_p = 1.21$ and 1.04, for plane and round plumes. It should be observed that these measurements verify that $K_w \approx 0.132$ and 0.11 for plane and round buoyant jets, constant from jet-like to plume-like behaviour. It is also evident that λ_B and λ can be iteratively calculated using (2.20) and (2.21) as functions of the local Richardson number R, which is known at a particular axial distance for given values of μ, m and β, or equivalently for w_m and c_m, assigning λ_B and λ values from a previous iteration. Therefore, to enable the calculation of λ_B and λ employing these functions, the FOA solutions given below for $\lambda_M = \lambda_B = 1$ are implemented in order to find a first approximation of R; this in turn serves for the determination of the values of λ_B, λ and a new R. The procedure converges quickly, requiring only three iterations, as the second value of R coincides with the correct R. All results in the present study have been obtained using simple programming in Microsoft Excel, without noticeable runtime required. In the case of the FOA, turbulent contributions in momentum and tracer fluxes are ignored, thus $\lambda_M = \lambda_B = 1$. YN and NY have defined the parameter γ as,

$$\gamma = \left(\frac{K_w^2 + K_c^2}{K_w}\right)^{(1+i)/2} \tag{2.22}$$

and based on centreline mean axial velocity and mean concentration measurements, NY have found that the variations of γ and the concentration spreading coefficient K_c were small; this finding has also been verified by an extended review of the literature. Consequently, constant values of $\gamma = 0.24$ and $K_c \approx 0.12$ have been considered pertinent for practical applications in round buoyant jets. Analysis of experimental data for a plane buoyant jet obtained by Kotsovinos (1975), made by YN in conjunction with extended reviews, has indicated again that γ and K_c remain essentially constant and the values $\gamma \approx 0.6$ and $K_c = 0.173$ have been suggested for use in practical applications for the entire buoyancy region.

Consideration of (2.19) and (2.22) yields,

$$\gamma \cong (2K_c)^{(1+i)/2}, \tag{2.23}$$

which interprets the physical significance and behaviour of γ; this equation connects present and previous findings, which are in complete agreement for both plane and round buoyant jets. For the FOA when $\lambda_M = \lambda_B = 1$, use of (2.19) and (2.23) into (2.13) gives:

$$f\left(Z^{(1+i)/2}\right) \cong \gamma Z^{(1+i)/2}. \tag{2.24}$$

It should be noted that the spreading parameters calculated by NY and YN, which satisfy the conservation constraints, enhance an effect due to omission of the turbulent flux contribution in the integral momentum and mass conservation equations and therefore values obtained by these workers differ slightly from those measured

Parameter	Plane Jet	Plane Plume	Round Jet	Round Plume	Equation
First-order approach (FOA)					
λ_M	1.0	1.0	1.0	1.0	
λ_B	1.0	1.0	1.0	1.0	(2.20)
$\lambda = K_c/K_w$	1.31	1.31	1.20	1.00	(2.21)
K_w	0.132	0.132	0.100	0.120	
K_c	0.173	0.173	0.120	0.120	(2.21)
Second-order approach (SOA)					
λ_M	1.1	1.1	1.1	1.1	
λ_B	1.04	1.18	1.076	1.15	(2.20)
$\lambda = K_c/K_w$	1.50	1.21	1.23	1.04	(2.21)
K_w	0.132	0.132	0.110	0.110	
K_c	0.198	0.160	0.135	0.114	(2.21)

TABLE 3. Values of input parameters involved in application of FOA and SOA for plane and round turbulent buoyant jets.

directly using more accurate techniques (Ramaprian & Chandrasekhara 1985, 1989; Papanicolaou & List 1988; Wang & Law 2002). Recommended input values to be assigned to parameters regarding turbulent flux contribution and spreading rates for the FOA and SOA integral models proposed in this paper are summarized in table 3.

2.4. *Final integration in the ZEF*

In the more general case of a SOA, factors λ_M and λ_B are calculated as previously described and accurate integral calculation based on equations (2.13) is employed; however, in the case of an FOA, when the concentration spreading coefficient K_c might be considered constant and factors $\lambda_M = \lambda_B = 1$, the integral function $F(Z^{(3+i)/2})$ could be determined with the aid of (2.24) and taken as:

$$F\left(Z^{(3+i)/2}\right) \cong \frac{2\gamma}{3+i} Z^{(3+i)/2}. \tag{2.25}$$

In addition, defining the profile of the tracer or buoyancy flux $T \equiv wc$ according to (2.6) (where T replaces ϕ), computing flux β and adopting (2.19), it is found that $\beta = \lambda_B(\sqrt{\pi}\, b_T)^{1+i} g_0' w_m c_m \cong \lambda_B(\sqrt{\pi b_w b_c/2})^{1+i} g_0' w_m c_m$. Thus, for the FOA, the nominal width of the tracer or buoyancy flux may be estimated on the basis of velocity and concentration widths b_w and b_c according to the following relationship:

$$b_T \cong \sqrt{\frac{b_w b_c}{2}}. \tag{2.26}$$

2.5. *Centreline axial velocity and concentration distributions*

The proposed solutions are provided in forms similar to those given by NY for round buoyant jets and YN for plane buoyant jets, in order to facilitate direct comparison. In synoptic presentation and irrespective of the variation of b_w and K_w with z, these solutions are:

$$\frac{w_m}{w_0} F_0^{2(1+i)/(3+i)} = \frac{2^{-i/2}}{\sqrt{\lambda_M}} \left(\frac{\pi}{2}\right)^{(i-1)/4} (K_w Z)^{-(1+i)/2} \left[M_1 + \tfrac{3}{2} 2^{i/2} \left(\frac{\pi}{2}\right)^{(1-i)/4} F\left(Z^{(3+i)/2}\right)\right]^{1/3} \tag{2.27}$$

$$c_m F_0^{2(1+i)/(3+i)} = \left(\frac{\pi}{4}\right)^{(i-1)/2} \lambda_B^{-1} (2K_w K_c)^{-(1+i)/2}\, Y Z^{-(1+i)} \left[\frac{w_m}{w_0} F_0^{2(1+i)/(3+i)}\right]^{-1}, \quad (2.28)$$

where $Z=(z/D)F_0^{-4/(3+i)}$, $F_0=w_0(g_0'D)^{-1/2}$, $Y=[(1+\lambda^2)/(2\lambda)]^{(1+i)/2}$ and $\lambda=K_c/K_w$; it should also be noted that

$$\frac{\sqrt{m_0}}{z^{(1+i)/2} w_m} = \frac{(\pi/4)^{i/2}}{Z^{(1+i)/2}} \left[\frac{w_m}{w_0} F_0^{2(1+i)/(3+i)}\right]^{-1},$$

$$\frac{\mu_0}{z^{(1+i)/2} c_m \sqrt{m_0}} = \frac{(\pi/4)^{i/2}}{Z^{(1+i)/2}} \left[c_m F_0^{2(1+i)/(3+i)}\right]^{-1}.$$

The functions $F(Z^{(3+i)/2})$ and M_1 are given by equations (2.13) and approximations (2.15) and (2.16). The spreading rate coefficients K_w, K_c, λ and the coefficients λ_M and λ_B are presented in table 3 in conjunction with (2.20) and (2.21). In the case of an FOA, when $\lambda_M=\lambda_B=1$, owing to approximations (2.19), (2.23), (2.24) and (2.25), solutions (2.27) and (2.28) are explicit and constitute simple analytical expressions defining uniquely the axial velocity and concentration distributions along the centreline of a plane and round buoyant jet; they were produced as a result of direct integration of the governing differential equations of momentum and tracer in conjunction with experimental evidence. These solutions, can also be employed to boost second-order solutions using (2.27) and (2.28) with the aid of (2.13), (2.15), (2.16), (2.20) and (2.21) and selecting from table 3 pertinent values of coefficients involved, as follows:

For plane buoyant jets ($i=0$) and M_1 as given by (2.15); for SOA $K_w=0.132$, $K_c=\lambda K_w$, $\lambda_M \approx 1.1$ and factors λ_B and λ as given by (2.20) and (2.21), respectively; for FOA $\lambda_M=\lambda_B=1$, $K_w=0.132$, $K_c=0.173$ (table 3).

For round buoyant jets ($i=1$) and M_1 as given by (2.16); for SOA, $K_w=0.11$, $K_c=\lambda K_w$, $\lambda_M \approx 1.1$ (table 3) and factors λ_B and λ as given by (2.20) and (2.21), respectively; for FOA $\lambda_M=\lambda_B=1$ and K_w as given by the empirical relationship $K_w=0.12-0.02\exp(-0.05Z^2)$ suggested by NY.

It must be noted that the solution for the mean concentration distribution in the centreline of round buoyant jets is qualitatively similar to the semi-empirical expressions proposed by Kotsovinos (1978, 1985) for mean centreline excess temperatures of turbulent round plumes. However, considering the experimental measurements initially reported by Noutsopoulos, Hatzicomninou & Yiannopoulos (1979) and later by NY, the relationships proposed by Kotsovinos underestimate the centreline concentrations by more than 15 % in the plume-like region and even more in the jet-like region.

The forms and coefficients of the limiting cases of the centreline mean axial velocities and mean concentrations for round and plane buoyant jets are presented in table 4. The analytical solutions given by the functional forms (2.27) and (2.28) are compared in figures 2(a) and 2(b), giving the centreline mean axial velocity and mean concentration distributions of a plane buoyant jet and in figures 3(a) and 3(b) showing similar data for a round buoyant jet. It should be noted that, without loss of generality, the FOA and SOA solutions illustrated in these figures concern specific values of the initial Froude number (i.e. $F_0=$ 2.5, 25, 50 and 100 or greater) for non-dimensional axial distances $z/D \geqslant 7$. Under these conditions, the effect of the ZFE on the ZEF behaviour is enhanced in the M_1 parameter and becomes noticeable, as the solutions deviate from the standard curves taken for $M_1=1$ (or large values of F_0). These curves correspond to the limit line, where curves of different Froude number tend to coincide; this line is termed standard behaviour and is characterized

Jet-like flows ($Z \to 0$)				Plume-like flows ($Z \to \infty$)			
Velocities		Concentrations		Velocities		Concentrations	
$\frac{w_m}{w_0} = A_j \left(\frac{z}{D}\right)^{-\delta_j}$		$c_m = B_j \left(\frac{z}{D}\right)^{-\sigma_j}$		$\frac{w_m}{w_0} = A_p F_0^{-2/3} \left(\frac{z}{D}\right)^{-\delta_p}$		$c_m = B_p F_0^{2/3} \left(\frac{z}{D}\right)^{-\sigma_p}$	
A_j	δ_j	B_j	σ_j	A_p	δ_p	B_p	σ_p
Plane ($i = 0$)							
$\left(\lambda_M \sqrt{\frac{1}{2}\pi K_{wj}}\right)^{-1/2}$	$\frac{1}{2}$	$\frac{\lambda_M^{1/2} Y_j}{\lambda_{Bj}} \left(\sqrt{\frac{1}{2}\pi K_{cj}}\right)^{-1/2}$	$\frac{1}{2}$	$\left(\frac{2Y_p}{\sqrt{\pi}} \frac{\sqrt{K_{cp}}}{\lambda_M \lambda_{Bp}}\right)^{1/3} K_{wp}^{-1/2}$	0	$\left(\frac{\lambda_M}{\lambda_{Bp}^2} \frac{Y_p^2 \sqrt{2}}{\pi K_{cp}^2}\right)^{1/3}$	1
Round ($i = 1$)							
$\frac{\sqrt{2}}{2K_{wj}\sqrt{\lambda_M}}$	1	$\frac{Y_j \sqrt{2\lambda_M}}{2\lambda_{Bj} K_{cj}}$	1	$\left(\frac{3K_{cp} \cdot Y_p}{4\lambda_M \lambda_{Bp}}\right)^{1/3} K_{wp}^{-1}$	$\frac{1}{3}$	$\left(\frac{\lambda_M \cdot Y_p^2}{6\lambda_{Bp}^2 K_{cp}^4}\right)^{1/3}$	$\frac{5}{3}$

TABLE 4. Forms of the centreline axial velocities and centreline concentrations in the limiting cases of plane and round turbulent buoyant jets. Subscripts j and p denote values at jet- or plume-like behaviour, respectively.

by a completely lost memory of initial buoyant jet characteristics transferred by M_1. Comparison between the FOA and SOA solutions proposed herein would show that, as expected, there are only quantitative differences. Figures 2(a) and 2(b) show that the FOA solution compared to the SOA solution for $z/D \geqslant 7$ over-predicts mean axial velocities and mean concentrations along the plane buoyant jet centreline from about 4 % and 2 % in the jet-like region up to 10 % and 5 % in the plume-like region, respectively. Similarly, figures 3(a) and 3(b) show that the FOA solution compared to the SOA solution over-predicts mean axial velocities and mean concentrations along the round buoyant jet centreline from about 15 % and 13 % in the jet-like region down to −2 and 0 % in the plume-like region, respectively.

An overall assessment of the proposed SOA behaviour for round buoyant jets is made in figures 4(a) and 4(b), where the SOA distributions of mean axial velocities and mean concentrations along the jet centreline are compared to empirical second-order approximations given by Wang & Law (2002) and experimental measurements conducted by Papanicolaou & List (1988) for velocities and Papanicolaou & List (1987) for concentrations. These distributions fit well with the experimental data and actually coincide with the results of the empirical model, since over-predictions less than 5 % and 9 % are observed for velocities and concentrations, respectively. Because of lack of adequate reliable velocity and concentration data for plane buoyant jets, an overall assessment of the proposed SOA behaviour for plane buoyant jets, will be made in a later section regarding bulk dilution, together with an additional confirmation of the findings for round buoyant jets.

Comparing the proposed expressions for the FOA solutions to corresponding values reported by YN and NY, for plane and round buoyant jets, respectively, it is observed that the data coincide both qualitatively and quantitatively. The empirical constant γ defined and determined by YN and NY using experimental axial velocity and concentration measurements ($\gamma \approx 0.6 \pm 0.053$ and $\gamma = 0.24 \pm 0.0157$ (mean $\pm$ standard deviation) for plane and round buoyant jets, respectively) should be replaced by the corresponding quantities $\sqrt{2K_c} = \sqrt{2 \times 0.173} \cong 0.59$ and $2K_c = 2 \times 0.12 = 0.24$, according to approximation (2.23). Therefore, the physical

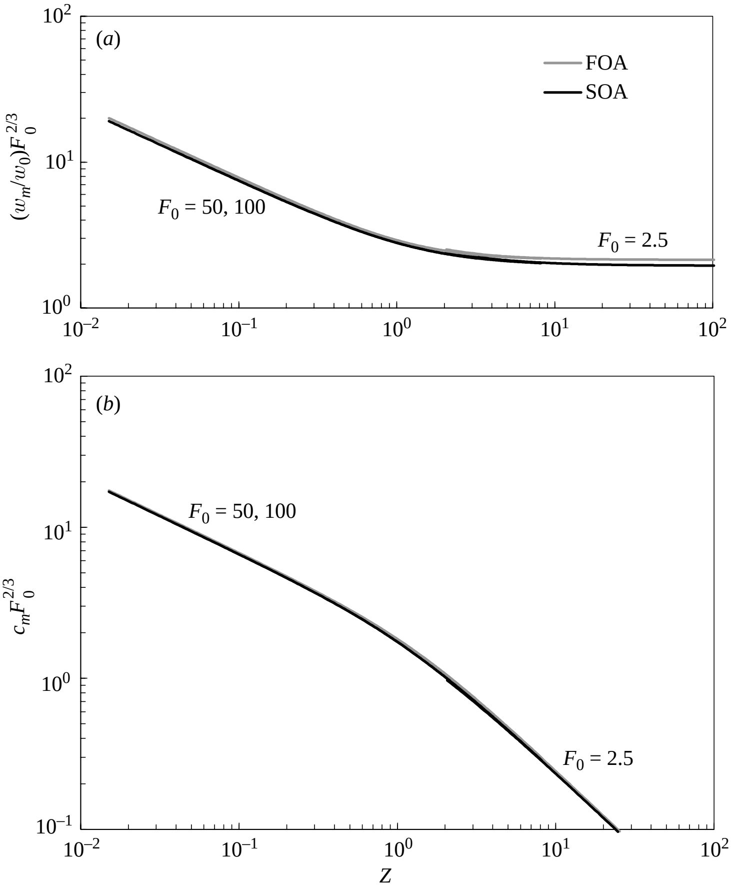

FIGURE 2. Plane buoyant jets: normalized centreline distributions of (a) mean axial velocity and (b) mean concentration, as functions of $Z = (z/D)\,F_0^{-4/3}$ and F_0 using FOA and SOA solutions.

significance of γ is delineated by the proposed FOA procedure, which constitutes an improved modification of the integration procedure and leads to exactly the same findings; it should be noted that YN and NY have made an extensive comparison of the limiting behaviour of the above expressions with other works reported in the literature and have concluded that an overall agreement existed.

An estimate of the accuracy of the proposed FOA and SOA solutions in the limiting behaviours can additionally be made by computing the relative difference of each proposed parameter A and B value from the related average value derived from measurements found in the literature; studies conducted in the last two decades using advanced techniques, which yielded more reliable data, are used. These differences are then normalized by dividing them with the latter average value, which is assumed to be *a priori* correct, and the result that gives a measure of the errors made is expressed as a percentage and presented in table 5 for plane jets and plumes and in table 6 for round jets and plumes. An evolution of the values given in tables 5 and 6 confirms that the SOA solutions are more accurate than the FOA solutions, as their maximum relative deviations from experimental average values remain less than 7.4 % compared to 14.2 % for the FOA solutions. However, both solutions have

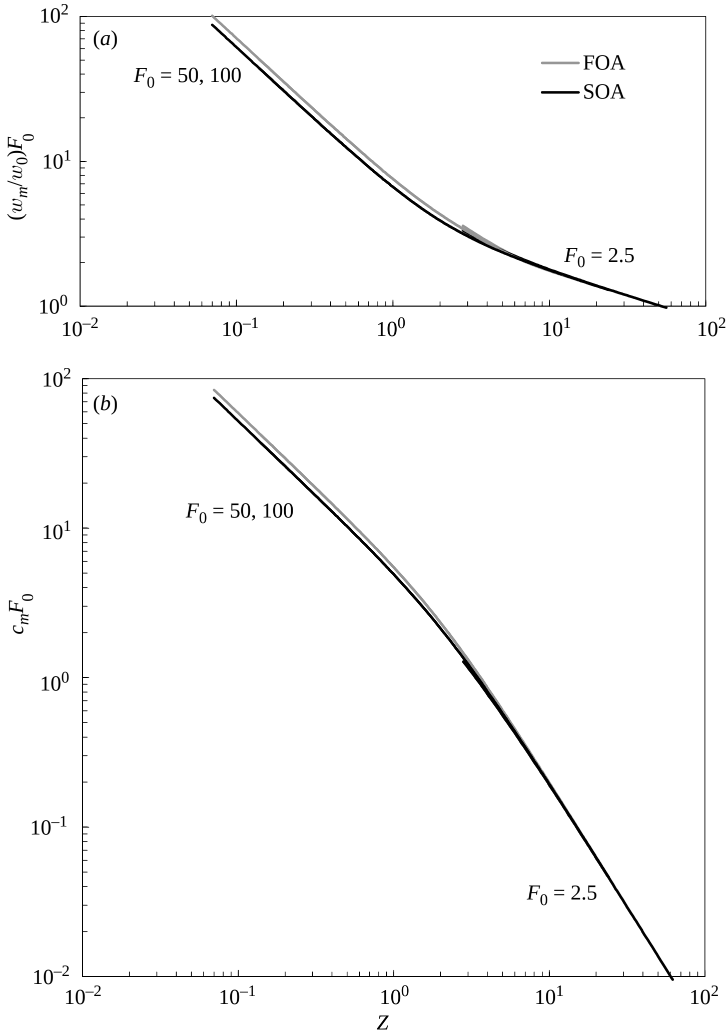

FIGURE 3. Round buoyant jets: normalized centreline distributions of (*a*) mean axial velocity and (*b*) mean concentration, as functions of $Z = (z/D)\,F_0^{-1}$ and F_0 using FOA and SOA solutions.

maximum absolute errors less than 10 % for plane jets and plane and round plumes, and only for round jets do the FOA solutions deviate more than 10 %.

3. Application to relevant quantities

Equations (2.27) and (2.28), which concern the centreline axial velocity and concentration distributions for the turbulent round and plane buoyant jet, will be used in the following sections for the determination of the variation of the local Richardson and Froude numbers, bulk dilution, dilution ratio, entrainment coefficient, transverse component of mean velocity and kinetic energy flux for the mean motion.

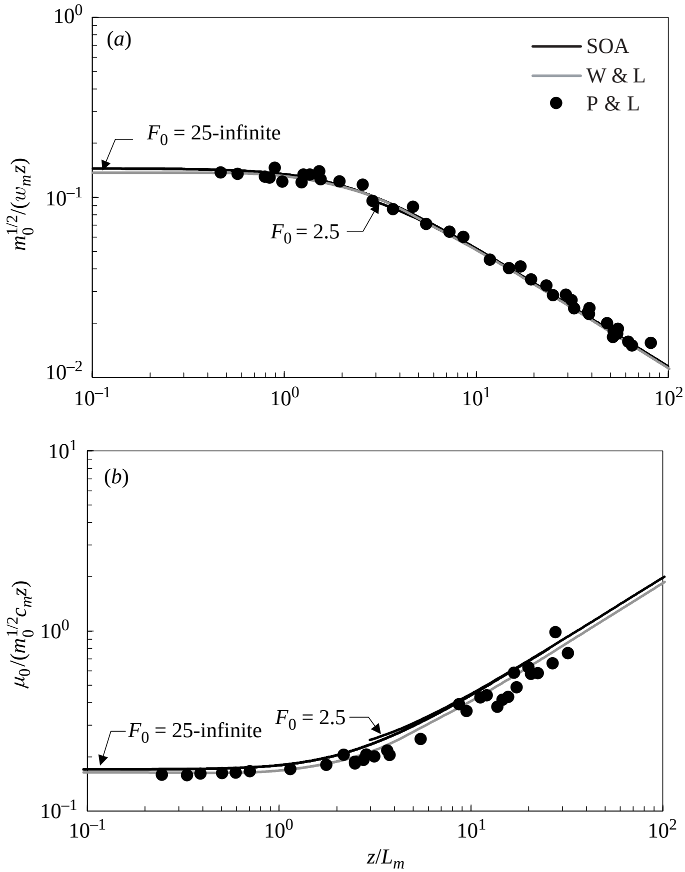

FIGURE 4. Round buoyant jets: normalized centreline distributions of (*a*) mean axial velocity and (*b*) mean concentration, as functions of $z/L_m = (\pi/4)^{-1/4} Z$ and F_0 using SOA solutions compared to the empirical second-order model by Wang & Law (2002) (W&L) and experimental measurements by Papanicolaou & List (1987, 1988) (P&L).

3.1. *Local Richardson and Froude numbers*

Applying dimensional analysis, the following general relationship for the local Richardson number for plane and round buoyant jets is obtained,

$$R = \frac{\mu^{(3+i)/(1+i)}\beta}{m^{(3+2i)/(1+i)}} \tag{3.1}$$

where $\mu = (\sqrt{\pi}\, b_w)^{1+i} w_m$, $m = \lambda_M(\sqrt{\pi/2}\, b_w)^{1+i} w_m^2$ and $\beta = \lambda_B(\pi b_w b_c/2)^{(1+i)/2} g_0' w_m c_m/Y$ are the volume, momentum, and buoyancy fluxes. By substituting these fluxes in (3.1), introducing the centreline velocity and concentration variables from (2.27) and (2.28), and making pertinent manipulations, the following final form is derived for the local Richardson number:

$$R = \lambda_M^{-(3+i)/2/(1+i)} \left(\frac{2}{\sqrt{\pi}}\right)^i (\sqrt{2\pi}\ K_w Z)^{(3+i)/2} \left[M_1 + \tfrac{3}{2} 2^{i/2} \left(\tfrac{1}{2}\pi\right)^{(1-i)/4} F\left(Z^{(3+i)/2}\right)\right]^{-1}. \tag{3.2}$$

Author	Jet A_j	Jet B_j	Jet D(cm)	Jet $Re \times 10^{-3}$	Plume A_p	Plume B_p
Present study						
FOA	2.46	2.15			2.14	2.47
Derivation from experimental average value (%)	7.7	4.9			2.6	2.1
SOA	2.34	2.11			1.94	2.42
Derivation from experimental average value (%)	2.5	2.9			−7.0	0.0
Experimentally measured values						
Ramaprian & Chandrasekhara (1985)	2.44	2.27	0.50	1.5		
Ramaprian & Chandrasekhara (1989)					2.13	2.56
Thomas & Chu (1989)	2.13		1.27	8.3		
Dracos *et al.* (1992)	2.28		1.00	10		
Yuan & Cox (1996)					2.04	2.60
Sangras, Dai & Faeth (1998)						2.10
Chen & Jirka (1999)		1.83	1.00	10		
Average value	2.28	2.05			2.09	2.42

TABLE 5. Evaluation of parameter A and B values for plane turbulent buoyant jets based on experiments conducted during the last two decades.

Author	Jet A_j	Jet B_j	Jet D(cm)	Jet $Re \times 10^{-3}$	Plume A_p	Plume B_p
Present study						
FOA	7.07	5.89			3.73	9.30
Derivation from experimental average value (%)	10.1	14.2			1.4	−2.5
SOA	6.13	5.20			3.71	9.32
Derivation from experimental average value (%)	−4.6	0.8			0.8	−2.3
Experimentally measured values						
Papanicolaou & List (1987)		5.37	0.75–2.00	1.7–17		9.46
Papanicolaou & List (1988)	6.71		0.75	1.8–11	3.55	
Dahm & Dimotakis (1990)		5.40	0.25	1.5–20		
Panchapakesan & Lumley (1993)	6.06		0.61	11		
Weisgraber & Liepmann (1998)	6.67		2.54	16		
Webster *et al.* (2001)	6.20	5.00	0.31	3.0		
Wang & Law (2002)	6.48	5.26	0.45–0.94	6.0–13	3.81	9.62
Tian & Roberts (2003)		5.00	0.40	2.6		
Average value	6.42	5.16			3.68	9.54

TABLE 6. Evaluation of parameter A and B values for round turbulent buoyant jets based on experiments conducted during the last two decades.

For both FOA and SOA solutions and for either plane or round buoyant jets, the variation of the local Richardson number R with respect to z/L_m is shown in figures 5(a) and 5(b), respectively. It is observed that both models produce comparable results and the maximum FOA overestimation compared to SOA results is about 16 % for both plane and round buoyant jets. In addition, for round buoyant jets, R is compared to the corresponding variation given by Wang & Law (2002), which

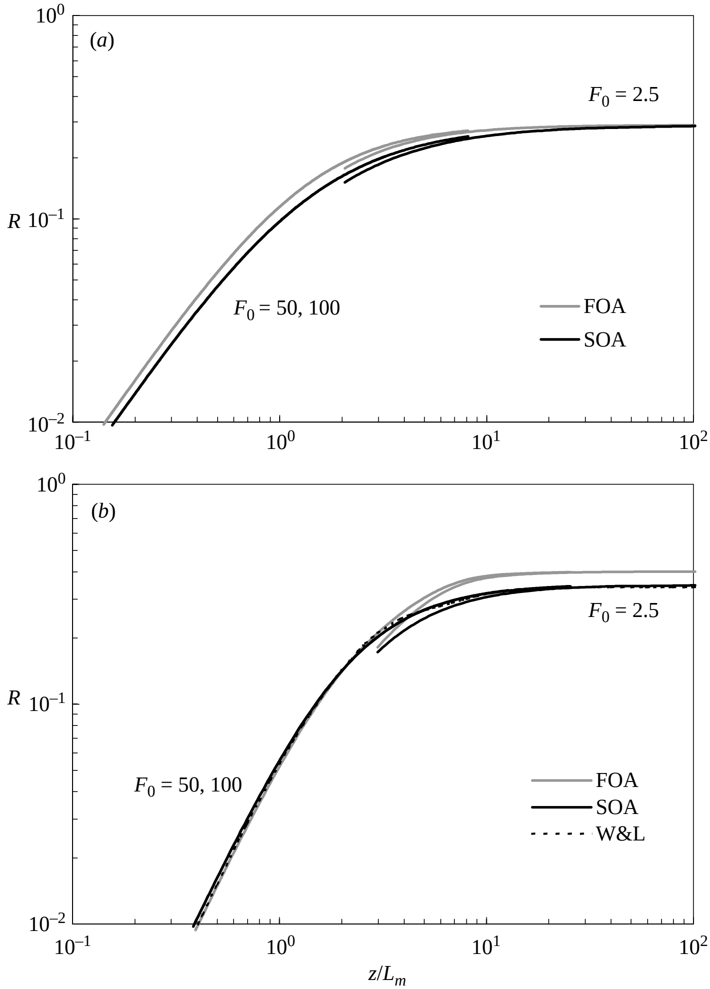

FIGURE 5. Local Richardson number R as a function of z/L_m and F_0 using FOA and SOA solutions for (a) plane buoyant jets and (b) round buoyant jets compared to the empirical second-order model by Wang & Law (2002) (W&L).

agrees very well with both proposed variations in the jet-like region and especially with R obtained by the SOA in the plume-like region. The limiting value R_p of the Richardson number in the plume-like case is taken from (3.2) for $Z \to \infty$:

$$R_p = \lambda_{Bp} \lambda_M^{-(2+i)/(1+i)} Y_p^{-1} \frac{3+i}{3} \sqrt{2\pi} \frac{K_{wp}}{\lambda_p^{(1+i)/2}}, \tag{3.3}$$

where index p denotes values at the plume-like behaviour. The jet-like behaviour of the Richardson number is taken for $Z \to 0$ and $M_1 = 1$ as,

$$R_j = \lambda_M^{-(3+i)/2/(1+i)} \left(\frac{2}{\sqrt{\pi}} \right)^i (\sqrt{2\pi}\, K_{wj} Z)^{(3+i)/2}, \tag{3.4}$$

where index j denotes values for jet-like behaviour. The local Richardson and Froude numbers are linked together through the following relationship:

$$RF^2 = \lambda_B \lambda_M^{-(3+2i)/(1+i)} Y^{-1} 2^{i/2} \sqrt{\pi}\, \lambda^{(1+i)/2}, \tag{3.5}$$

and the local Froude number F is defined on the jet centreline in accordance to the initial Froude number,

$$F = \frac{w_m}{\sqrt{g'_m 2b_w}} \tag{3.6}$$

where $g'_m = g'_0 c_m$ is the local apparent acceleration due to gravity; and $2b_w$ is the local nominal width of the flow field used instead of the exit size D in the initial Froude number. For plumes, the limiting values of the local Richardson and Froude numbers, using (3.3) and (3.5) with parameter values from table 3, are:

plane buoyant jet

FOA	$R_p = 0.2891$	and	$F_p = 2.65$,
SOA	$R_p = 0.2907$	and	$F_p = 2.43$,

round buoyant jet

FOA	$R_p = 0.4011$	and	$F_p = 2.50$,
SOA	$R_p = 0.3521$	and	$F_p = 2.59$.

Physically, the limiting R_p or F_p values reflect the equilibrium condition of buoyant to inertial forces. At this location, the initially accelerated plume has obtained its maximum axial velocity, while it is decelerated downstream. For plane plumes, the values of R_p, determined on the basis of the proposed solutions, are found to be about equal to the value $R_p = 0.28 \pm 0.04$ determined by Ramaprian & Chandrasekhara (1989). The corresponding value based on measurements by Kotsovinos (1975) and reported by Fischer *et al.* (1979) is $R_p = 0.735^{3/2} = 0.63$; this value is about twice as great as the value given by Ramaprian & Chandrasekhara (1989) and might have resulted from systematic measurement errors in the plane plume region causing a considerable velocity underestimation (see also figure 6 in YN). For round plumes, the values of R_p, determined on the basis of the proposed solutions, are found to be very close to the value $R_p = 0.584^2 = 0.341$ determined by Wang & Law (2002), slightly larger than the value $0.557^2 = 0.310$ proposed by Fischer *et al.* (1979), and considerably lower than the value $0.716^2 = 0.513$ determined by Papanicolaou & List (1988). However, Papanicolaou & List (1988), noting that the technique used for concentration measurements had introduced systematic errors yielding about 22 % [(0.09 − 0.07)/0.09] lower values, made a correction according to their previous concentration measurements (Papanicolaou & List 1987), and calculated a new value $R_p = (0.716 \times 0.07/0.09)^2 = 0.557^2 = 0.310$; the revised value coincides with the value proposed by Fischer *et al.* (1979).

3.2. *Dispersion ratio*

The concentration-to-velocity width ratio or dispersion ratio is defined according to (2.21) for either plane or round buoyant jets, and the limiting values of λ that are used in (2.21) for both approaches are given in table 3. It is noted that for the FOA of round buoyant jets, K_w is given by the empirical relationship $K_w = 0.12 - 0.02\exp(-0.05Z^2)$ suggested by NY. For both approximations, the variation of λ with respect to R is given in figures 6(a) and 6(b) for plane and round buoyant jets, respectively. The variation of λ is independent of the F_0 variation for plane buoyant jets, but depends on F_0 for round buoyant jets using FOA data only. For plane buoyant jets, the SOA shows appreciable differences in λ (from 8 % to 12 %) from the FOA for increasing

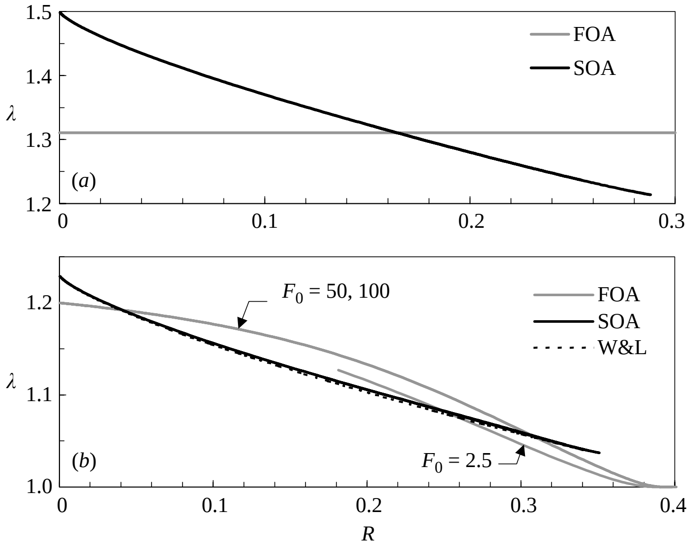

FIGURE 6. Variation of the concentration-to-velocity width ratio λ as a function of R and F_0 using FOA and SOA solutions with F_0 varied from 2.5 to infinity for (a) plane buoyant jets and (b) round buoyant jets compared to values by Wang & Law (2002) (W&L).

R. For round buoyant jets, both approaches show comparable values of λ, which are also quite close to the values given by Wang & Law (2002) (the maximum differences are less than 3 %). Chu, Lee & Chu (1999) have determined experimentally the value of $\lambda = 1.2$ for a turbulent round jet in coflow, which coincides with the value obtained herein by the FOA for round jets and is very close to that given by the SOA.

3.3. *Bulk dilution*

The bulk dilution can be defined as,

$$S = \frac{\mu}{\mu_0}, \tag{3.7}$$

where $\mu = (\sqrt{\pi}\, b_w)^{1+i} w_m$ and $\mu_0 = (\pi/4)^i D^{1+i} w_0$. After substituting these fluxes into (3.7) and taking into consideration equations (2.27) and (2.28), the bulk dilution can be expressed as,

$$\left.\begin{aligned} S F_0^{-2(1+i)/(3+i)} &= \left(\frac{2}{\lambda}\right)^{(1+i)/2} \frac{Y}{\lambda_B}\left[c_m F_0^{2(1+i)/(3+i)}\right]^{-1}, \\ \text{or, equivalently,} \qquad S &= \left(\frac{2}{\lambda}\right)^{1+i/2} \frac{Y}{\lambda_B} c_m^{-1}, \end{aligned}\right\} \tag{3.8}$$

where $i = 0$ for plane buoyant jets and $i = 1$ for round buoyant jets. The variation of the bulk dilution with respect to Z is shown in figures 7(a) and 7(b) for plane and round buoyant jets, respectively; it compares well with experimental data available in the literature and seems to be independent of the M_1 variation. The maximum FOA overestimations from SOA results observed are about 10 % and 19 % for plane and round buoyant jets, respectively; in addition, the bulk dilution obtained using the SOA solutions compares better to experimental measurements reported by Kotsovinos &

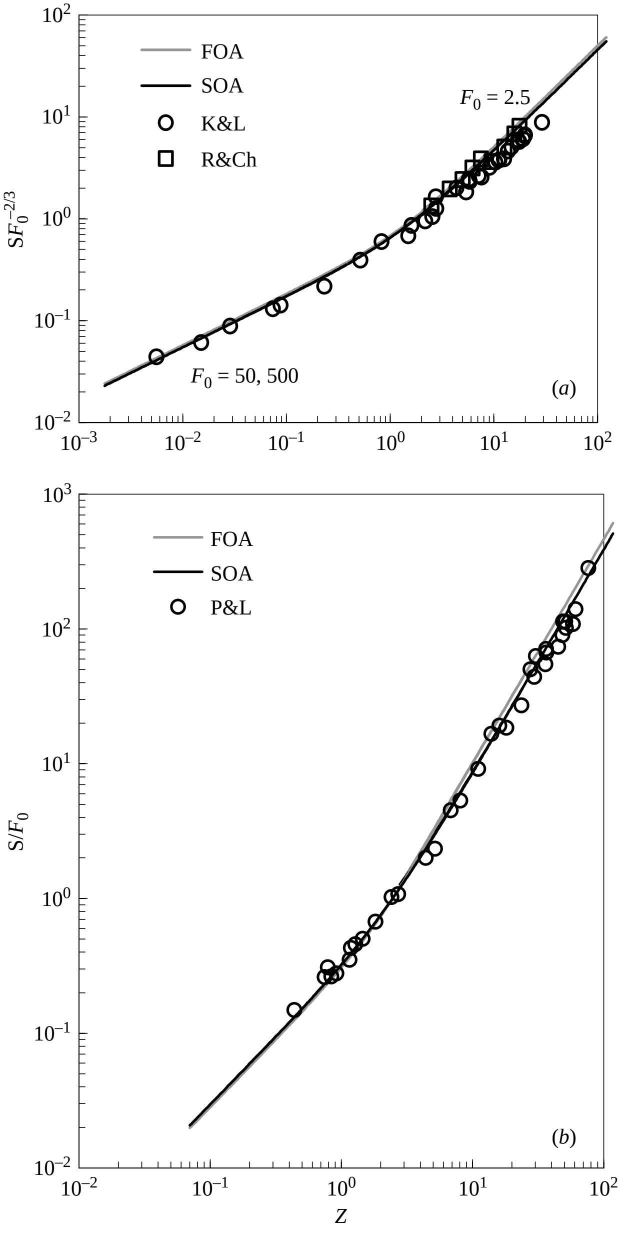

FIGURE 7. Normalized bulk dilution as a function of Z and F_0 using FOA and SOA solutions with F_0 varied from 2.5 to 500 for (*a*) plane buoyant jets compared to experimental measurements by Kotsovinos & List (1977) (K&L) and Ramaprian & Chandrasekhara (1983) (R&Ch) and (*b*) round buoyant jets compared to experimental measurements by Papanicolaou & List (1988) (P&L).

List (1977) and Ramaprian & Chandrasekhara (1983) for plane buoyant jets and by Papanicolaou & List (1988) for round buoyant jets.

The limiting forms of the bulk dilution for plane and round buoyant jets are given in table 7. In conjunction with parameter values given in table 3, the values computed

Parameter description	Plane ($i=0$)	Round ($i=1$)
Jet-like flows ($Z \to 0$)		
Bulk dilution, $S_j =$	$(2\pi)^{1/4}\left(\dfrac{K_{wj}}{\lambda_M}\right)^{1/2}\left(\dfrac{z}{D}\right)^{1/2} = \Gamma_j\left(\dfrac{z}{D}\right)^{1/2}$	$2\left(\dfrac{2}{\lambda_M}\right)^{1/2} K_{wj}\dfrac{z}{D} = \Gamma_j\dfrac{z}{D}$
Dilution ratio, $\left(\dfrac{c_m}{C_{av}}\right)_j =$	$\dfrac{Y_j}{\lambda_{Bj}}\left(\dfrac{2}{\lambda_j}\right)^{1/2}$	$\dfrac{2Y_j}{\lambda_{Bj}\lambda_j}$
Entrainment coefficient, $a_j =$	$\dfrac{\sqrt{\pi}}{4}K_{wj}$	$\dfrac{K_{wj}}{2}$
Kinetic energy for the mean flow, $\varepsilon_j =$	$\left(\dfrac{8}{\pi}\right)^{1/4}\dfrac{\lambda_M^{-3/2}}{\sqrt{3K_{wj}}}\left(\dfrac{z}{D}\right)^{-1/2}\varepsilon_0$	$\dfrac{\sqrt{2}}{3K_{wj}}\lambda_M^{-3/2}\left(\dfrac{z}{D}\right)^{-1}\varepsilon_0$
Plume-like flows ($Z \to \infty$)		
Bulk dilution, $S_p =$	$\left(\dfrac{2\pi Y_p\sqrt{\lambda_p}}{\lambda_M\lambda_{Bp}}\mathrm{K}_{wp}^2\right)^{1/3} F_0^{-2/3}\dfrac{z}{D} = \Gamma_p F_0^{-2/3}\dfrac{z}{D}$	$\left(\dfrac{48Y_p\lambda_p}{\lambda_M\lambda_{Bp}}\mathrm{K}_{wp}^4\right)^{1/3} F_0^{-2/3}\left(\dfrac{z}{D}\right)^{5/3} = \Gamma_p F_0^{-2/3}\left(\dfrac{z}{D}\right)^{5/3}$
Dilution ratio, $\left(\dfrac{c_m}{C_{av}}\right)_p =$	$\dfrac{Y_p}{\lambda_{Bp}}\left(\dfrac{2}{\lambda_p}\right)^{1/2}$	$\dfrac{2Y_p}{\lambda_{Bp}\lambda_p}$
Entrainment coefficient, $a_p =$	$\dfrac{\sqrt{\pi}}{2}K_{wp}$	$\dfrac{5}{6}K_{wp}$
Kinetic energy for the mean flow, $\varepsilon_p =$	$\dfrac{Y_p}{\sqrt{3}}\dfrac{\sqrt{\lambda_p}}{\lambda_M\lambda_{Bp}}\beta_0 z = E_p\beta_0 z$	$\dfrac{Y_p\lambda_p}{2\lambda_M\lambda_{Bp}}\beta_0 z = E_p\beta_0 z$
f-kinetic energy term for the mean flow, $\varepsilon_{fp} =$	$[1+(a_pA_p)^3 - E_p]\beta_0 = E_{fp}\beta_0$	$\left[1+\frac{4}{0.18^2}(a_pK_{wp}A_p)^3 - E_p\right]\beta_0 = E_{fp}\beta_0$

TABLE 7. Forms of several parameters in the limiting cases for plane and round turbulent buoyant jets. Subscripts j and p denote values at jet- or plume-like behaviour, respectively; $\varepsilon_0 = \beta_0 F_0^2 D/2$.

are for plane jets ($i=0$, $Z \to 0$) $\Gamma_j =$ 0.575 and 0.548 and for plane plumes ($i=0$, $Z \to \infty$) $\Gamma_p =$ 0.500 and 0.454 for the FOA and SOA solutions, respectively. Fischer *et al.* (1979) have suggested $\Gamma_j = 0.5 \pm 0.02$ for plane jets, which is very close to the present findings, and a rather underestimated value $\Gamma_p = 0.34$ for plane plumes. Similarly, the values are for round jets ($i=1$, $Z \to 0$) $\Gamma_j =$ 0.283 and 0.297 and for round plumes ($i=1$, $Z \to \infty$) $\Gamma_p =$ 0.215 and 0.179 for the FOA and SOA solutions, respectively. Fischer *et al.* (1979) have suggested $\Gamma_j = 0.25 \pm 0.001$ for round jets and $\Gamma_p = 0.15 \pm 0.015$ for round plumes, which are somewhat lower than the values obtained in the present study. Papanicolaou & List (1988) have measured $\Gamma_j = 0.284$ for pure round jets and $\Gamma_p = 0.164$ for round plumes, in very close agreement with the predictions by the proposed SOA. It is noted that the parameters Γ_j and Γ_p are defined in table 7 for each particular case.

3.4. *Dilution ratio*

The dilution ratio is defined according to Fischer *et al.* (1979) as,

$$\frac{c_m}{C_{av}} = \frac{c_m}{c_0} S, \tag{3.9}$$

where $C_{av} = c_0\mu_0/\mu = c_0/S$ and $c_0 = 1$ for the present work. Substituting c_m from (2.28) and S from (3.7), (3.9) finally results in the simple relationship,

$$\frac{c_m}{C_{av}} = \frac{Y}{\lambda_B}\left(\frac{2}{\lambda}\right)^{(1+i)/2}, \tag{3.10}$$

which can be further simplified in dedicated forms for:

plane buoyant jets ($i = 0$)

$$\frac{c_m}{C_{av}} = \frac{Y}{\lambda_B}\left(\frac{2}{\lambda}\right)^{1/2}, \tag{3.11}$$

round buoyant jets ($i = 1$)

$$\frac{c_m}{C_{av}} = \frac{2Y}{\lambda_B \lambda}. \tag{3.12}$$

The limiting forms of the dilution ratio for plane and round buoyant jets are given in table 7. In conjunction with parameter values given in table 3, the values computed are for plane jets ($i = 0$, $Z \rightarrow 0$) $(c_m/C_{av})_j =$ 1.24 and 1.16 and for plane plumes $(c_m/C_{av})_p =$ 1.24 and 1.10 for the FOA and SOA solutions, respectively, and, as can be seen, the dilution ratio obtained by each approach remains constant for the entire buoyancy region. Related values suggested by Fischer *et al.* (1979) are 1.2 ± 0.1 for plane jets and 0.81 ± 0.1 for plane plumes; however, the latter value which was based on the Kotsovinos (1975) measurements was characterized by Fischer *et al.* (1979) as a ‘curious result’, and these measurements underestimated significantly the axial velocities and bulk dilution (figure 7*a*). Values computed for round jets ($i = 1$, $Z \rightarrow 0$) are $(c_m/C_{av})_j =$ 1.67 and 1.54 and for round plumes $(c_m/C_{av})_p =$ 2.00 and 1.67 for FOA and SOA solutions, respectively. These values are higher than the value 1.4 ± 0.1 suggested by Fischer *et al.* (1979) for both cases, however, data by Papanicolaou & List (1988) support present findings well enough, as they give $c_m/C_{av} =$ 1.71 and 1.70 for round jets and plumes, respectively. The experimentally determined value of Chu *et al.* (1999) for a turbulent round jet in coflow is about 1.66, while Roberts, Snyder & Baumgartner (1989) measured the value of 2.0 for a three-dimensional diffuser field of mixing in a current.

3.5. *Entrainment coefficient*

The entrainment coefficient can be evaluated by the continuity equation (2.7), introducing the ‘jet entrainment hypothesis’ established by Morton *et al.* (1956), according to which,

$$u_e = -\,a w_m, \tag{3.13}$$

where a is the entrainment coefficient; substituting u_e into (2.7), the following relationship is obtained:

$$\frac{d\mu}{dz} = \frac{d}{dz}\left[\left(\sqrt{\pi} b_w\right)^{1+i} w_m\right] = 2(\pi\, b_w)^i a w_m. \tag{3.14}$$

Solving (3.14) for a and making pertinent manipulations, the following expression results:

$$a = \frac{1+i}{2}\pi^{(1-i)/2}\frac{\mathrm{d}b_w}{\mathrm{d}z} + \tfrac{1}{2}\pi^{(1-i)/2}\frac{b_w}{w_m}\frac{\mathrm{d}w_m}{\mathrm{d}z} = \tfrac{1}{2}\pi^{(1-i)/2}K_w\,(1+i+s_i), \tag{3.15}$$

where the logarithmic slope of the centreline decay of the mean axial velocity s_i is derived using (2.27) and (3.2) and has the following form:

$$s_i = \frac{z}{w_m}\frac{\mathrm{d}w_m}{\mathrm{d}z} = -\frac{1+i}{2} + \frac{\lambda_M^{(2+i)/(1+i)}}{2\sqrt{2\pi}\lambda_B K_w} Y\lambda^{(1+i)/2}R. \tag{3.16}$$

Substituting for s_i, (3.15) yields:

$$a = \frac{1+i}{4}\pi^{(1-i)/2}K_w\left[1 + \frac{1}{(1+i)\sqrt{2\pi}}\frac{\lambda_M^{(2+i)/(1+i)}}{\lambda_B K_w}Y\lambda^{(1+i)/2}R\right]. \tag{3.17}$$

The limiting forms of the entrainment coefficient for plane and round buoyant jets are given in table 7. In conjunction with the parameter values given in table 3, the values computed are for plane jets ($i=0$, $Z\to 0$) $a_j=0.0585$ and for plane plumes ($i=0$, $Z\to\infty$) $a_p=0.117$ for both the FOA and SOA solutions. Similarly, the values for round jets ($i=1$, $Z\to 0$) are $a_j=$ 0.050 and 0.055, and for round plumes ($i=1$, $Z\to\infty$) $a_p=$ 0.100 and 0.0917 for the FOA and SOA solutions, respectively.

For the variation of a with respect to R, Kotsovinos & List (1977) have suggested that,

$$a = a_j - (a_j - a_p)\frac{R}{R_p}, \tag{3.18}$$

where a_j and a_p refer to the jet-like and plume-like behaviour. Owing to the dependence of λ_B and λ on R, (3.17) implies that a is a nonlinear function of R and therefore (3.18) should be considered as an approximation only. This would mean that the integral models, which use the closing assumption of the entrainment hypothesis (assuming that a is proportional to R), introduce *a priori* an inconsistency. The SOA solution gives less than 4 % and 9 % lower values of a compared to FOA for plane and round buoyant jets, respectively, and the deviations of SOA a values from data given by Wang & Law (2002) are less than 15 %.

3.6. *Transverse component of mean velocity*

Assuming that the transverse distribution of the axial velocity component is described well enough by the Gaussian profile (2.6), continuity equation (2.1) can be integrated in the transverse direction from 0 to r, giving:

$$\frac{u}{w_m} = K_w[(1+i+s_i)I_i n^{-i} - n\exp(-n^2)], \tag{3.19}$$

where s_i is the logarithmic slope of the centreline decay of the mean axial velocity defined by (3.16), $I_0=\int_0^n \exp(-t^2)\,\mathrm{d}t$, $I_1=[1-\exp(-n^2)]/2$ and $n=r/b_w$. Equation (3.19) gives analytically the profiles of the transverse component of mean velocity and is valid for the entire buoyancy range and for plane and round vertical buoyant jet geometries. Plots of these profiles are shown in figures 8(a) and 8(b) for plane and round buoyant jets, respectively, and, in each diagram, results obtained using the FOA and SOA solutions are plotted.

For plane jets when $s_0=-1/2$, (3.19) results qualitatively in exactly the same form as the forms reported by Dracos, Giger & Jirka (1992) and Agrawal & Prasad (2003).

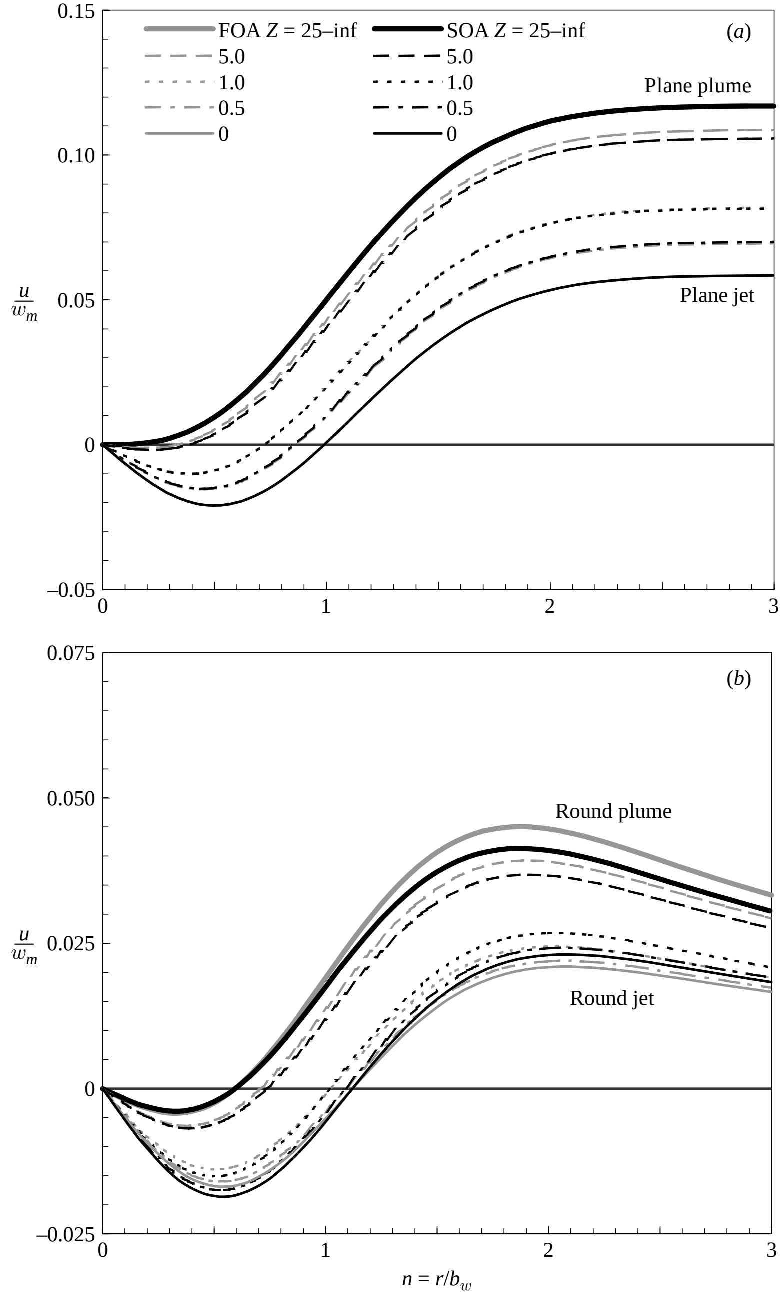

FIGURE 8. Transverse distributions of the transverse component of mean velocity normalized by the centreline axial velocity component as function of n and Z using FOA and SOA solutions for (a) plane buoyant jets and (b) round buoyant jets.

For plane plumes when $s_0 = 0$, (3.19) again results in the same form as derived by Agrawal & Prasad (2003), but these investigators have used the value $K_w = 0.11$ instead of 0.132 used herein; therefore, transverse velocities are underestimated by 20 %, compared to the present predictions. Finally, the FOA and SOA predictions compared to each other coincide almost completely with a maximum deviation of less than 3 %.

For round jets when $s_1 = -1$, and round plumes when $s_1 = -1/3$, (3.19) results qualitatively in exactly the same forms as the related forms reported by Ying *et al.* (2004) and Agrawal & Prasad (2003); and the FOA and SOA predictions compared to each other show small differences (up to 9 %).

3.7. *Kinetic energy flux for the mean motion*

The kinetic energy flux for the mean motion ε, normalized by its initial value ε_0 at the jet exit, is,

$$\frac{\varepsilon}{\varepsilon_0} = \left(\frac{4}{3}\right)^i \left(\frac{\pi}{3}\right)^{(1-i)/2} \lambda_E \left(\frac{b_w}{D}\right)^{1+i} \left(\frac{w_m}{w_0}\right)^3 \tag{3.20}$$

and the factor λ_E can be computed by the formula:

$$\lambda_E = 1 + \frac{\displaystyle\int_A (w/w_m)(u/w_m)^2\,\mathrm{d}A}{\displaystyle\int_A (w/w_m)^3\,\mathrm{d}A}, \tag{3.21}$$

where u is the transverse component of mean velocity. The distributions of the cross-stream velocity have been given in the preceding section and after conducting pertinent computations using these distributions, it was found that λ_E varies in the range from 1 to 1.00226 for plane buoyant jets and from 1 to 1.00144 for round buoyant jets; thus, the value of $\lambda_E = 1$ can be used. Therefore, (3.20) with the aid of (2.27) finally results in the form:

$$\frac{\varepsilon}{\varepsilon_0} F_0^{2(1+i)/(3+i)} = \left(\frac{4}{3}\right)^i \left(\frac{\pi}{3}\right)^{(1-i)/2} K_w^{1+i} Z^{1+i} \left[\frac{w_m}{w_0} F_0^{2(1+i)/(3+i)}\right]^3. \tag{3.22}$$

The variation of the normalized kinetic energy flux for the mean motion is plotted with respect to Z and for several values of F_0 in figures 9(a) and 9(b), for plane and round buoyant jets, respectively. The maximum FOA overestimations compared to SOA results are about 35 % and 27 % for plane and round buoyant jets, respectively. It can be observed from these figures that the kinetic energy flux has its minimum value at the regions of Z from 0.9 to 1.1 and from 2.1 to 2.4, for plane and round buoyant jets, respectively. The limiting behaviours of the kinetic energy flux are of considerable interest, and the limiting forms of the normalized kinetic energy flux for the mean motion for plane and round buoyant jets are presented in table 7. In the plume limiting case, the gradient of the kinetic energy flux normalized by the initial value of the buoyancy flux β_0 is constant, as follows:

plane plumes ($i = 0$, $Z \to \infty$)

$$\frac{\mathrm{d}\varepsilon_p}{\beta_0 \mathrm{d}z} = E_p = \frac{Y_p}{\sqrt{3}} \frac{\sqrt{\lambda_p}}{\lambda_M \lambda_{Bp}}, \tag{3.23}$$

round plumes ($i = 1$, $Z \to \infty$)

$$\frac{\mathrm{d}\varepsilon_p}{\beta_0 \mathrm{d}z} = E_p = \frac{Y_p \lambda_p}{2\lambda_M \lambda_{Bp}}, \tag{3.24}$$

where $\beta_0 = 2\varepsilon_0 F_0^{-2} D^{-1}$. In conjunction with the parameter values given in table 3, the values computed are for plane plumes ($i = 0$, $Z \to \infty$) $E_p =$ 0.661 and 0.494,

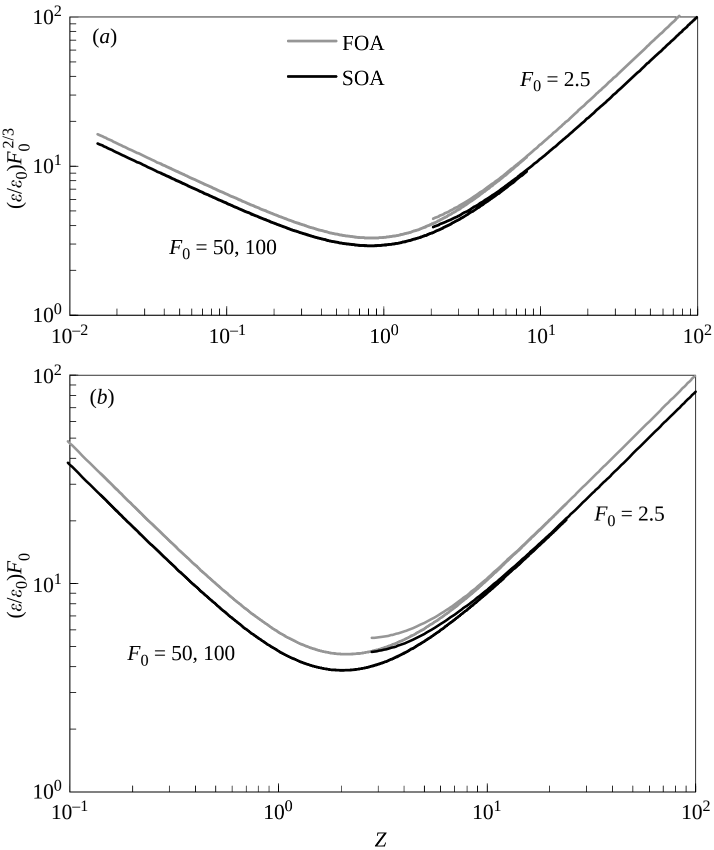

FIGURE 9. Normalized kinetic energy flux of the mean motion as a function of Z and F_0 using FOA and SOA solutions with F_0 varied from 2.5 to 100 for (*a*) plane buoyant jets and (*b*) round buoyant jets.

and for round plumes ($i = 1$, $Z \to \infty$) $E_p =$ 0.500 and 0.411 for the FOA and SOA results, correspondingly. In a neutral environment, Turner (1972) has reported the computational values $E_p =$ 0.578 and 0.500 for line and axisymmetric plumes, while Rouse *et al.* (1952) have measured $E_p =$ 0.53 and 0.57 for plane and round plumes, respectively. It should be observed that the values of E_p remain approximately equal for round or plane plumes, as their difference is only about 17 % according to present SOA data and 7.5 % according to experimental results by Rouse *et al.* (1952).

Taking into consideration the conservation of the mean kinetic energy equation (2.10), the flux of the f-kinetic energy terms normalized by β_0 can be calculated by the following equations:

plane plumes

$$\frac{\varepsilon_f}{\beta_0} = 1 + \left[a\left(\frac{w_m}{w_0}F_0^{2/3}\right)\right]^3 - \frac{\mathrm{d}\varepsilon}{\beta_0 \mathrm{d}z}, \tag{3.25}$$

round plumes

$$\frac{\varepsilon_f}{\beta_0} = 1 + \frac{4}{0.18^2}K_w^3 Z\left[a\left(\frac{w_m}{w_0}F_0\right)\right]^3 - \frac{\mathrm{d}\varepsilon}{\beta_0 \mathrm{d}z}. \tag{3.26}$$

Based on (3.25) and (3.26) and using the corresponding plume-like forms for velocity and entrainment coefficient (tables 4 and 7) and (3.23) and (3.24), E_{fp} (defined in table 7) values were computed and show that the flux of the f-kinetic energy terms is also conserved in the plume limiting case. For plane plumes, these values are $E_{fp} =$ 0.355 and 0.518, and for round plumes $E_{fp} =$ 0.511 and 0.595 for the FOA and SOA solutions, respectively.

Another convenient relationship with general implications can be obtained by using the definition of ε given in table 1 in conjunction with the definition of the local Richardson number given by (3.1) and taking into account that $\beta = \beta_0 = 2\varepsilon_0 F_0^{-2} D^{-1}$ for plane and round buoyant jets. After pertinent arrangements the following formula is taken:

$$\frac{\varepsilon R}{\beta_0 z} = p, \tag{3.27}$$

where $p = \sqrt{2\pi}\, 2^i 3^{-(1+i)/2} \lambda_M^{-(3+2i)/(1+i)} K_w$. It is obvious that p is constant as both λ_M and K_w are constants. Substituting the pertinent values for the FOA given in table 3, values of $p = 0.191$ for plane buoyant jets and $p =$ 0.167 and 0.201 for round jets and plumes, respectively, are computed. After assigning λ_M and K_w values for the SOA, $p = 0.144 \pm 0.0008$ is obtained for both plane and round buoyant jets, which means that it might be a universal constant. As the SOA gives the most reliable results, the constant value $p = 0.144$ is adopted for (3.27) and by careful observation the following significant implications can be deduced:

(i) The product $\varepsilon R/z$ is a conservative quantity for both plane and round buoyant jets.

(ii) In the limiting plume case, where R equals to a constant R_p, both quantities ε/z and $\mathrm{d}\varepsilon/\mathrm{d}z$ are conserved.

(iii) Equation (3.27) constitutes an alternative definition of the local Richardson number and has the advantage that this definition obeys a common law independent from the two-dimensional or three-dimensional geometrical properties of the flow and mixing field.

A universal definition of the local Richardson number may therefore be proposed:

$$R \equiv p\frac{\beta\, z}{\varepsilon}, \tag{3.28}$$

where $p = 0.144$ is a universal constant, β and ε the local buoyancy and kinetic energy fluxes for the mean motion, and z the vertical distance from the jet exit. According to this definition, the Richardson number compares locally the work done by the buoyant force with the flux of the kinetic energy for the mean motion. Finally, it should be noted that the property of conservation of the ratio of kinetic energy flux over distance z or the gradient of kinetic energy flux for the mean motion have found significant use in the solution of the multiple buoyant jet problem by extending the application of the superposition method in the region of plume-like flows (Yannopoulos 1996; Yannopoulos & Bekri 2003; Yannopoulos & Noutsopoulos 2005).

4. Summary and conclusions

Theoretical analysis was based on the four partial differential equations of continuity, momentum, tracer and kinetic energy for the mean motion written on the basis of acceptable simplifications for such types of flow. These equations are given in a unified way for both plane and round turbulent buoyant jets discharged vertically upwards in a stagnant ambient fluid being a little denser than the jet fluid. The integral method, in conjunction with the experimentally well-supported assumption of Gaussian profiles for velocity and concentration, was used to reduce the partial differential equations to a set of four ordinary differential equations, including the variable second-order effect of turbulence on the mean momentum and tracer fluxes according to Wang & Law (2002). The jet-spreading approach, initially used by Abraham (1963), was employed to integrate the differential equations. The basic closing assumption that γ, a function of spreading coefficients defined by (2.22), is independent of distance z, initially adopted by NY for round buoyant jets and implemented by YN in plane buoyant jets, is physically explained and enhanced in the present work. According to (2.23), function γ is proportional to the square root of the spreading coefficient K_c for plane buoyant jets and simply to K_c for round buoyant jets, or equivalently to $\sqrt{\lambda K_w}$ and λK_w, with a maximum error 4 %; and since recent experimental measurements demonstrate that the spreading coefficient K_w remains constant, function γ becomes, respectively, proportional to $\sqrt{\lambda}$ and λ. The variation of concentration-to-velocity width ratio or dispersion ratio λ can only be ignored when the FOA is implemented. In addition, present findings concerning function γ actually imply that the mass (or tracer) spreading rate for plane and round buoyant jets is approximately equal to the geometric mean of velocity and concentration spreading rates divided by $\sqrt{2}$. Under this assumption and related approximations, the equations of momentum and tracer were directly integrated, taking into consideration the proper boundary conditions due to the ZFE, and this led to explicit analytical expressions concerning the dimensionless centreline axial velocities and concentrations in a unified way for both plane and round buoyant jets. The two analytical expressions, (2.27) and (2.28), constitute solution approximations of either first or second order, depending on the values and functional forms of the coefficients assigned; suggested values have been given in table 3. The SOA solution requires the corresponding FOA analytical solution to estimate an initial value of the Richardson number, which in turn is used for the computation of all necessary parameters that depend on this number. Applying iteratively this procedure for only three iterations yields the correct value of the Richardson number and this leads to a converged SOA solution. The corresponding FOA and SOA solutions compare well to each other, while comparisons to experimental measurements available in the literature show very good agreement for $z/D \geqslant 7$, with errors being less that 9 %. The FOA and SOA solutions applied for computing the suggested coefficients (table 3) are validated for their overall end-effect behaviour, expressed through the predicted limiting values of A and B, by comparing them to corresponding average values of experimentally measured data during the last two decades, which are available in the literature and are summarized in tables 5 and 6 for plane and round buoyant jets, respectively. The maximum absolute errors made by using the FOA and SOA are 14.2 % and 7 %, hence, the proposed SOA model accomplished the presupposition for errors less than 10 %.

The validated solutions have been used in order to compute the variation of the local Richardson and Froude numbers and the dispersion ratio; again, the SOA findings show better agreement with available data based on experimental measurements. Values herein proposed for plume-like behaviour based on the SOA solution are $R_p = 0.2907$ and 0.3521, $F_p = 2.43$ and 2.59, for plane and round plumes, respectively; the dispersion ratio λ varies from jets to plumes in the corresponding ranges 1.50 to 1.21 and 1.23 to 1.04 for plane and round buoyant jets, while the empirical expressions adopted gave reasonable results. In addition, the proposed solutions in conjunction with the integral equations of continuity and kinetic energy for the mean motion have been employed to determine the variation of bulk dilution, dilution ratio, entrainment coefficient, transverse component of mean velocity, kinetic energy flux, f-terms flux for the mean motion and the product of kinetic energy flux and the local Richardson number, as well as the variation of the gradient of these kinetic energy fluxes. Based on the SOA solution, the proposed variation of the dilution ratio from jets to plumes is $c_m/C_{av} =$ 1.16 to 1.10 and 1.54 to 1.67, for plane and round buoyant jets, respectively; the entrainment coefficient a varies in the ranges of 0.0585 to 0.117 and 0.055 to 0.0917, while analytical functions for the profiles of the transverse component of velocity for plane and round buoyant jets are given.

Particular attention was paid to the variation of the kinetic energy flux gradient for the mean motion and especially the product of kinetic energy flux and the local Richardson number. This product, divided by the initial buoyancy flux β_0 and by the distance z, is found to be a universal constant equal to 0.144 both for plane and round buoyant jets. Conservation of both the kinetic energy flux divided by the distance z and the gradient of the kinetic energy flux was found in the plume-like region, for either plane or round plumes. A universal definition of the local Richardson number, in a unique way irrespective of flow and mixing geometries, is proposed as $R \equiv p\beta z/\varepsilon$. The new physical insight obtained by this work, in terms of the universal conserved definition of R, can have a far-reaching implication to the future analysis of buoyant-jet problems.

REFERENCES

Abraham, G. 1963 Jet diffusion in stagnant ambient fluid. *Tech. Rep.* 29. Delft Hydraulics Lab., Delft.

Agrawal, A. & Prasad, A. K. 2003 Integral solution for the mean flow profiles of turbulent jets, plumes, and wakes. *Trans. ASME* I: *J. Fluids Engng* **125**, 813–822.

Albertson, M. L., Dai, Y. B., Jensen, R. & Rouse, H. 1950 Diffusion of submerged jets. *Trans. ASCE* **115**, 639–664.

Chen, D. & Jirka, G. H. 1999 LIF study of plane jet bounded in shallow water layer. *J. Hydraul. Engng ASCE* **125**, 817–826.

Chu, P. C. K., Lee, J. H. & Chu, V. H. 1999 Spreading of turbulent round jet in coflow. *J. Hydraul. Engng ASCE* **125**, 193–204.

Dahm, W. J. A. & Dimotakis, P. E. 1990 Mixing at large Schmidt number in the self-similar far field of turbulent jets. *J. Fluid Mech* **217**, 299–330.

Davidson, M. J., Gaskin, S. & Wood, I. R. 2002 A study of a buoyant axisymmetric jet in a small co-flow. *J. Hydraul. Res.* **40**, 477–489.

Dracos, T., Giger, M. & Jirka, G. H. 1992 Plane turbulent jets in a bounded fluid layer. *J. Fluid Mech.* **241**, 587–614.

Fischer, H. B., List, E. J., Koh, R. C. Y., Imberger, J. & Brooks, N. H. 1979 *Mixing in Inland and Coastal Waters*. Academic.

Jirka, G. H. 2004 Integral model for turbulent buoyant jets in unbounded stratified flows. Part I: Single round jet. *Envir. Fluid Mech.* **4**, 1–56.

Jirka, G. H., Abraham, G. & Harleman, D. R. F. 1975 An assessment of techniques for hydrothermal prediction. *Tech. Rep.* R75-31, No. 203. Ralph M. Parsons Lab., MIT, Cambridge, Massachusetts.

Jirka, G. H., Doneker, R. L. & Hinton, S. W. 1996 Users manual for CORMIX: A hydrodynamic mixing zone model and decision support system for pollutant discharges into surface waters. *Tech. Rep.* DeFrees Hydraulics Lab., Cornell University, Ithaca, New York.

Kotsovinos, N. E. 1975 A study of the entrainment and turbulence in a plane buoyant jet. *Tech. Rep.* KH-R-32. W. M. Keck Laboratory of Hydraulics and Water Resources, California Inst. of Technology, California.

Kotsovinos, N. E. 1978 Dilution in a vertical round buoyant jet. *J. Hydraul. Div. ASCE* **104**, 795–798.

Kotsovinos, N. E. 1985 Temperature measurements in a turbulent round plume. *Intl J. Heat Mass Transfer* **28**, 771–777.

Kotsovinos, N. E. & List, E. J. 1977 Plane turbulent buoyant jets. Part 1. Integral properties. *J. Fluid Mech.* **81**, 25–44.

Lee, J. H. W. & Cheung, V. 1990 Generalized Langrangian model for buoyant jets in current. *J. Envir. Engng ASCE* **116**, 1085–1106.

List, E. J. & Imberger, J. 1973 Turbulent entrainment in buoyant jets and plumes. *J. Hydraul. Div. ASCE* **99**, 1461–1474.

Morton, B. R. 1959 Forced plumes. *J. Fluid Mech.* **5**, 151–163.

Morton, B. R., Taylor, G. I. & Turner, J. S. 1956 Turbulent gravitational convection from maintained instantaneous sources. *Proc. R. Soc. Lond.* A **234**, 1–23.

Noutsopoulos, G., Hatzicomninou, S. & Yiannopoulos, P. 1979 Discussion of 'dilution in a vertical round buoyant jet' by N. E. Kotsovinos. *J. Hydraul. Div. ASCE* **104**, 629–631.

Noutsopoulos, G. & Yannopoulos, P. 1987 The round vertical turbulent buoyant jet. *J. Hydraul. Res.* **25**, 481–502 (referred to as NY).

Panchapakesan, N. R. & Lumley, J. L. 1993 Turbulence measurements in axisymmetric jets of air and helium. Part 1. Air jet. *J. Fluid Mech.* **246**, 197–223.

Papanicolaou, P. N. & List, J. E. 1987 Statistical and spectral properties of tracer concentration in round buoyant jets. *Intl J. Heat Mass Transfer* **30**, 2059–2071.

Papanicolaou, P. N. & List, J. E. 1988 Investigations of round vertical turbulent buoyant jets. *J. Fluid Mech.* **195**, 341–391.

Ramaprian, B. R. & Chandrasekhara, M. S. 1983 Study of vertical plane turbulent jets and plumes. *Tech. Rep.* IIHR 257. Iowa Institute of Hydraulic Research, the University of Iowa, Iowa.

Ramaprian, B. R. & Chandrasekhara, M. S. 1985 LDA measurements in plane turbulent jets. *Trans. ASME* I: *J. Fluids Engng* **107**, 264–271.

Ramaprian, B. R. & Chandrasekhara, M. S. 1989 Measurements in vertical plane turbulent plumes. *Trans. ASME* I: *J. Fluids Engng* **111**, 69–77.

Reichardt, H. 1941 On a new theory of free turbulence. *Z. Angew. Math. Mech.* **21**, 257–264, english translation in *J. R. Aeronaut. Soc.* (1943) **47**, 167–176.

Roberts, P. J. W., Snyder, W. & Baumgartner, D. J. 1989 Ocean outfalls. I: Submerged wastefield formation. *J. Hydraul. Engng ASCE* **115**, 1–25.

Rouse, H., Yih, C. & Humphreys, H. W. 1952 Gravitational convection from a boundary source. *Tellus* **4**, 201–210.

Sangras, R., Dai, Z. & Faeth, G. M. 1998 Mixing structure of plane self-preserving buoyant turbulent plumes. *Trans. ASME* J: *J. Heat Transfer* **120**, 1033–1041.

Shabbir, A. & George, W. K. 1994 Experiments on a round turbulent buoyant plume. *J. Fluid Mech.* **275**, 1–32.

Thomas, F. O. & Chu, H. C. 1989 An experimental investigation of the transition of a planar jet: subharmonic suppression and upstream feedback. *Phys. Fluids* A **1**, 1566–1587.

Tian, X. & Roberts, P. J. W. 2003 A 3D LIF system for turbulent buoyant jet flows. *Exps. Fluids* **35**, 636–647.

Turner, J. S. 1972 On the energy deficiency in self-preserving convective flows. *J. Fluid Mech.* **53**, 217–226.

Turner, J. S. 1986 Turbulent entrainment: the development of the entrainment assumption, and its application to geophysical flows. *J. Fluid Mech.* **173**, 431–471.

Wang, H. & Law, A. W.-K. 2002 Second-order integral model for a round turbulent buoyant jet. *J. Fluid Mech.* **459**, 397–428.

Webster, D. R., Roberts, P. J. W. & Ra'ad, L. 2001 Simultaneous DPTV/PLIF measurements of a turbulent jet. *Exps. Fluids* **30**, 65–72.

Weisgraber, T. H. & Liepmann, D. 1998 Turbulent structure during transition to self-similarity in a round jet. *Exps. Fluids* **24**, 210–224.

Wood, I. R., Bell, R. G. & Wilkinson, D. L. 1993 *Ocean Disposal of Wastewater*. World Scientific.

Yannopoulos, P. & Noutsopoulos, G. 1990 The plane vertical turbulent buoyant jet. *J. Hydraul. Res.* **28**, 565–580 (referred to as YN).

Yannopoulos, P. C. 1996 Superposition model for multiple plumes and jets predicting end effects. *J. Geophys. Res.* **101**, 15153–15167.

Yannopoulos, P. C. & Bekri, H. S. 2003 A modified virtual image source technique for multiple plume discharges into a flowing ambient. In *Proc. XXX IAHR Congress on Water Engineering and Research in a Learning Society: Modern Developments and Traditional Concepts* (ed. J. Ganoulis & P. Prinos), *Inland Waters: Research, Engineering and Management Theme*, (theme ed. C. I. Nezu & N. Kotsovinos), vol. 1, pp. 271–277. Aristotle University of Thessaloniki, Greece.

Yannopoulos, P. C. & Noutsopoulos, G. C. 2005 Interaction of vertical round turbulent buoyant jets. Part I: Entrainment restriction approach. Part II: Superposition method. *J. Hydraul. Res.* (in press).

Ying, C., Davidson, M. J., Wang, H. W. & Law, A. W.-K. 2004 Radial velocities in axisymmetric jets and plumes. *J. Hydraul. Res.* **42**, 29–33.

Yuan, L.-M. & Cox, G. 1996 An experimental study of some line fires. *Fire Safety J.* **27**, 123–139.